High-performance Silicon Arrayed-Waveguide Grating (De)multiplexer with 0.4-nm Channel Spacing

Xiaowan Shen
State Key Laboratory for Modern Optical Instrumentation
College of Optical Science and Engineering, Zhejiang University
Hangzhou, China
12130066@zju.edu.cn

Weike Zhao
State Key Laboratory for Modern Optical Instrumentation
College of Optical Science and Engineering, Zhejiang University
Hangzhou, China
wkzhao@zju.edu.cn

Huan Li
State Key Laboratory for Modern Optical Instrumentation
College of Optical Science and Engineering, Zhejiang University
Hangzhou, China
lihuan20@zju.edu.cn

Daoxin Dai
State Key Laboratory for Modern Optical Instrumentation
College of Optical Science and Engineering, Zhejiang University
Hangzhou, China
dxdai@zju.edu.cn

***Abstract*—We present a 0.4-nm channel spacing silicon arrayed-waveguide grating with Euler-bend-assisted broadened arrayed waveguides and shallowly-etched transition regions. For the present AWG, the excess loss is 0.65-3.11 dB and the crosstalk is below −18 dB.**

Keywords—Arrayed waveguide grating, silicon photonics, wavelength-division-multiplexing

I. Introduction

Silicon arrayed-waveguide gratings (AWGs) are crucial as a key element for high-capacity wavelength-division-multiplexing (WDM) systems [1]. As the demand for the link capacity of WDM systems continues to increase, it is desired to develop AWGs with many channels and very narrow channel spacing. However, the ultra-high index-contrast makes submicron silicon photonic waveguides very sensitive to random fabrication variations, which leads to significant random phase errors for light propagating along the arrayed waveguides. As a result, those compact silicon AWGs usually exhibit high excess loss and high inter-channel crosstalk particularly when designed with a very narrow channel spacing, as demonstrated previously [2-7]. We present a high-performance 32×32 AWG with 0.4-nm channel spacing for dense WDM systems, which is realized with a compact footprint of 900×2200 μm^2 by using 220-nm-thick silicon photonic waveguides. For the designed AWG, the arrayed waveguides are broadened to be far beyond the single-mode regime so that random phase errors and propagation loss are minimized even without any additional requirement for the fabrication processes. Furthermore, Euler-bends are introduced for the arrayed waveguides to shrink the device footprint and suppress any excitation of higher-order modes. Besides, shallowly-etched transition regions (SETRs) are inserted at the junction between the free-propagation regions (FPRs) and the arrayed waveguides in order to reduce the mode mismatch loss. For the fabricated AWG, the excess loss for the central channel is about 0.65 dB, the channel non-uniformity is about 2.5 dB, and the crosstalk is less than ~−18 dB. To our best knowledge, such an AWG is one of the best among silicon implementations, featuring dense channel spacing and high channel number.

This work was supported by National Major Research and Development Program (No. 2021YFB2801700/2021YFB2801702), National Science Fund for Distinguished Young Scholars (61725503), National Natural Science Foundation of China (NSFC) (91950205, 61961146003, 92150302, 62105283), Zhejiang Provincial Natural Science Foundation (LD19F050001), Zhejiang Provincial Major Research and Development Program (No. 2021C01199), Leading Innovative and Entrepreneur Team Introduction Program of Zhejiang (2021R01001), and the Fundamental Research Funds for the Central Universities..

II. Design and Fabrication

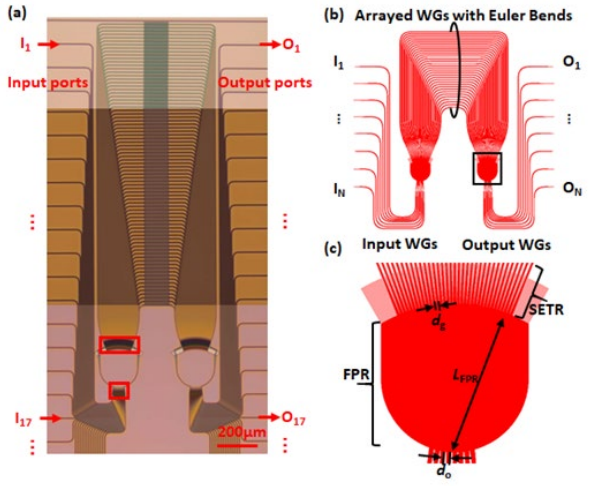

Fig. 1. a) Top view photograph of the fabricated 32×32 AWG; b) Schematic configuration of the designed AWG; c) Schematic configuration of the FPR and the SETR.

TABLE I. Parameters of the Designed AWG

Parameters	λ_0 (nm)	L_{FPR} (μm)	d_g (μm)	d_o (μm)	ΔL (μm)	*FSR* (nm)
Value	1550	200	1.6	1.84	43.84	14.6

With an SOI wafer with a 220-nm-thick top-silicon layer on a 2-μm-thick buried oxide layer, the designed AWGs were patterned by using an electron-beam lithography (EBL) process and an inductively coupled plasma (ICP) dry-etching

process. Finally, a 1.5-μm-thick SiO2 upper-cladding was deposited. Fig. 1 a) shows the top view photograph of the fabricated 32×32 AWG. The parameters of the AWG are chosen as shown in TABLE I. Fig. 1 b) and c) show the schematic configuration of the proposed compact silicon AWG with Euler-bend-assisted arrayed waveguides, which are designed specially with significantly broadened straight- and bent-sections as wide as e.g. 2μm (which is far beyond the single-mode condition). The effective index becomes less sensitive to the variation of the core width when the core width is larger, which is due to the less field amplitude at the waveguide sidewalls. As a result, it is expected that the random phase errors and the sidewall scattering loss of silicon photonic waveguides can be reduced greatly by significantly broadening the core width. In our previous work, it has been demonstrated that using broadened photonic waveguides is very helpful to greatly reduce the random phase errors in optical interference systems (like Mach-Zehnder interferometers [8]). On the other hand, one has to carefully manipulate the light propagation in arrayed waveguides which are far beyond the single-mode regime, in order not to excite the undesired higher-order modes. Here Euler bends are introduced for the arrayed waveguides to minimize higher-order mode excitation even with a small effective bending radius [9]. It is expected that using the present design with significantly broadened arrayed waveguides can greatly reduce the random phase errors from the fabrication imperfection. Accordingly, the channel crosstalk can be reduced greatly and the fabrication tolerance can also be improved.

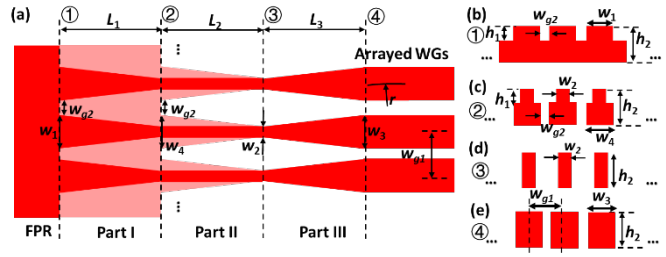

Fig. 2. a) Top view of the SETR; b) Cross section of the waveguide between FPR and Part I; c) Cross section of the waveguide between Part I and Part II; d) Cross section of the waveguide between Part II and Part III; e) Cross section of the waveguide between Part III and arrayed waveguides.

TABLE II. DESIGN PARAMETERS OF THE SETRS

Parameters	w_1	w_2	w_3	w_4	L_1	L_2	L_3
Value (μm)	1.4	0.45	2	1.6	21	30	27

Fig. 2 a) shows the top view of the SETRs, which consists of three Parts (i.e., I, II and III). Parts I and III are respectively based on shallowly-etched ridge waveguides and deeply-etched strip waveguides, as shown in Fig. 2 b)- e). Part II is for the adiabatic taper connecting part I and part III. Here we choose the shallowly-etching depth and the deeply-etching depth as h_1 = 70 nm and h_2 = 220 nm according to the definition from the foundry process. The minimal gap (w_{g2}) between adjacent arrayed waveguides is chosen as 200 nm according to the requirement of the foundry process. In order to connect the FPR and the arrayed waveguides, the width w_1 must be chosen meticulously in order to maximize the excitation of the fundamental mode in arrayed waveguides. Accordingly, the excitation of higher-order modes in arrayed waveguides is minimized. For part III, the end width w_3 is the same as the width of the Euler bends (which is far beyond the single-mode regime). Therefore, part II plays a key role to filter out the residual power of higher-order modes (which might be excited in part I of the arrayed waveguides). As a result, the end width w_2 for part II is chosen according to the single-mode condition so that higher-order modes are not allowed and can be removed. Furthermore, the end widths w_2 and w_4 of part II should be chosen carefully to avoid mode hybridization in the adiabatic tapers. Note that the lengths (L_1, L_2 and L_3) of parts I, II, and III should be chosen to satisfy the adiabatic condition for the fundamental mode propagation. The specific parameters of the SETRs designed for the transverse electric (TE) polarization are shown in TABLE II.

III. RESULTS AND DISCUSSIONS

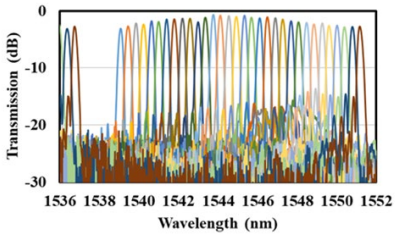

Fig. 3. Measured transmission spectrum for center input port.

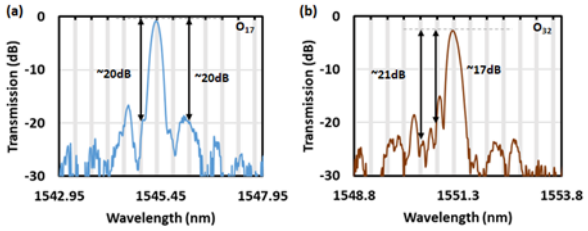

Fig. 4. a) The measured transmission spectrum of I_{17} to O_{17}; (b) The measured transmission spectrum of I_{17} to O_{32}..

The AWG is characterized in terms of excess loss and crosstalk. Fig. 3 shows the measured transmission spectra from the central input port (I_{17}). Here it was normalized with respect to the transmission of a 2-μm-wide straight waveguide with the same grating couplers on the same chip. It can be seen that the measured *FSR* is 14.6 nm and the measured channel-spacing is $\Delta\lambda_{ch}$ = 0.4 nm (i.e., Δf_{ch} = 50 GHz at 1550 nm), which agrees well with the design values. The transmission from the central input port to the central output port has an excess loss as low as 0.65 dB, owing to the introduction of the significantly broadened arrayed waveguides and the SETRs. On the other hand, the edge channels usually have higher excess loss than the central channel, depending on the envelop of the far field according to the principle of AWGs [11]. For the present AWG, the channel non-uniformity is about 2.5 dB, which should be improved further by choosing a long FPR or optimizing the distribution of the optical field exited from the arrayed waveguides. Fig. 4 a) shows the measured transmission spectra from the central input port (I_{17}) to the central output port (O_{17}). From this figure, one sees that the crosstalk between the adjacent channels is about −20 dB while the non-adjacent crosstalk is below −20 dB. In contrast, the results for those channels at the edge degrades in some degree due to the phase aberrations (which often occurs for AWGs [10]). For example, the measured transmission from port I_{17} to the output port O_{32} at the edge is shown in Fig. 4 b). It can be seen that the crosstalk between adjacent channels is about −17

dB and the non-adjacent crosstalk is below −21 dB. Therefore, more efforts should be made to improve the performance by compensating the aberration in the system.

IV. Conclusion

In summary, we present a high-performance 32×32 AWG with 0.4-nm channel spacing for dense WDM systems, using Euler-bend-assisted broadened arrayed waveguides and shallowly-etched transition regions. The measurement results show the fabricated AWG has an excess loss of 0.65 dB for the central channel, the channel non-uniformity is 2.5 dB, and crosstalk less than ∼−18 dB. Our demonstrated silicon AWG with a large channel number and narrow channel spacing shows superior performance among the reported silicon AWG, to the best of our knowledge. Such a high-performance AWG could play an important role in future optical interconnect and optical communication systems.

References

[1] K. Okamoto, “Progress and technical challenge for planar waveguide devices: silica and silicon waveguides,” Laser Photonics Rev., 2012, pp. 14-23

[2] X. Fu, D. Dai, “Ultra-small Si-nanowire-based 400 GHz-spacing 15 x 15 arrayed-waveguide grating router with microbends,” Electron. Lett., 2011, pp. 266.

[3] W. Bogaerts, S.K. Selvaraja, P. Dumon, J. Brouckaert, K. De Vos, D. Van Thourhout, R. Baets, “Silicon-on-Insulator Spectral Filters Fabricated With CMOS Technology,” IEEE J. Sel. Top. Quantum Electron., 2010, pp. 33-44.

[4] Q. Fang, T.-Y. Liow, J.F. Song, K.W. Ang, M. Bin Yu, G.Q. Lo, D.-L. Kwong, “WDM multi-channel silicon photonic receiver with 320 Gbps data transmission capability," Opt. Express, 2010, pp. 5106-5113.

[5] P. Dumon, W. Bogaerts, D. Van Thourhout, D. Taillaert, R. Baets, J. Wouters, S. Beckx, P. Jaenen, “Compact wavelength router based on a Silicon-on-insulator arrayed waveguide grating pigtailed to a fiber array,” Opt. Express, 2006, pp. 664-669.

[6] W. Bogaerts, P. Dumon, D. Van Thourhout, D. Taillaert, P. Jaenen, J. Wouters, S. Beckx, V. Wiaux, R.G. Baets, “Compact wavelength-selective functions in silicon-on-insulator photonic wires,” IEEE J. Sel. Top. Quantum Electron., 2006, pp. 1394-1401.

[7] Y. Shi, X. Fu, D. Dai, “Design and fabrication of a 200 GHz Si-nanowire-based reflective arrayed-waveguide grating (de)multiplexer with optimized photonic crystal reflectors,” Appl. Opt., 2010, pp. 4859-4865.

[8] L. Song, H. Li, D. Dai, “Mach-Zehnder silicon-photonic switch with low random phase errors,” Opt. Lett., 2021, pp. 78-81.

[9] X. Jiang, H. Wu, D. Dai, “Low-loss and low-crosstalk multimode waveguide bend on silicon,” Opt. Express, 2018, pp. 17680-17689.

[10] J. Zou, Z. Le, J. Hu, J.-J. He, “Performance improvement for silicon-based arrayed waveguide grating router,” Opt. Express, 2017, pp. 9963-9973.

[11] P. Dumon, W. Bogaerts, D. Van Thourhout, D. Taillaert, R. Baets, J. Wouters, S. Beckx, P. Jaenen, “Compact wavelength router based on a Silicon-on-insulator arrayed waveguide grating pigtailed to a fiber array,” Opt. Express, 2006, pp. 664-669.